# Whirl Flutter Studies for a SSTOL Transport Demonstrator

C. W. Acree, Jr.
Aerospace Engineer
NASA Ames Research Center
Moffett Field, CA
Cecil.W.Acree@nasa.gov

Krishna Hoffman
Engineer/Scientist
Boeing Phantom Works
Huntington Beach, CA
krishna.hoffman@boeing.com

## Abstract

A proposed new class of aircraft—the Advanced Theater Transport (ATT)—will combine strategic range and high payload with "Super-STOL" (short take-off and landing) capability. It is also proposed to modify a YC-15 into a technology demonstrator with a 20-deg tilt wing; four, eight-bladed propellers; cross-shafted gearboxes and V-22 engines. These constitute a unique combination of design features that potentially affect performance, loads and whirl-mode stability (whirl flutter). NASA Ames Research Center is working with Boeing and Hamilton Sundstrand on technology challenges presented by the concept; the purpose of NASA involvement is to establish requirements for the demonstrator and for early design guidance, with emphasis on whirl flutter. CAMRAD II is being used to study the effects of various design features on whirl flutter, with special attention to areas where such features differ from existing aircraft, notably tiltrotors. Although the stability margins appear to be more than adequate, the concept requires significantly different analytical methods, principally including far more blade modes, than typically used for tiltrotors.

## Notation

| | |
|---|---|
| ATT | Advanced Theater Transport |
| AMST | Advanced Manned Strategic Transport |
| IFPC | Integrated Flight/Prop Controls |
| OWE | Operating Weight Empty |
| SHP | Shaft Horsepower |
| SLS | Sea-Level Standard |
| SSTOL | Super-Short Take-Off and Landing |
| TOGW | Take-Off Gross Weight |
| VTOL | Vertical Take-Off and Landing |
| $f$ | frequency |
| M | Mach number |
| $r$ | radius (local) |
| $R$ | rotor radius |

## Introduction

The Advanced Theater Transport (ATT) concept combines strategic range and high payload with super-short take-off and landing (SSTOL) capability (Ref. 1). The key feature is a partially tilting wing with very large propellers to enable takeoff in 750 ft. As a technology demonstrator, a YC-15 would be modified to include the critical design features of the full-scale ATT (Ref. 2). Because its flight will occur sooner and its airframe aerodynamics and structure are already well-defined, the YC-15 SSTOL technology demonstrator is the focus of the present research. NASA is cooperating with the Boeing Company to investigate loads, performance, handling qualities, and aeroelastic stability of the demonstrator. The last of these research areas—aeroelastic stability, or whirl flutter—is the topic of this paper. CAMRAD II (Ref. 3) was used to study the effects of various design features on whirl flutter.

To provide background for the research, the ATT concept is briefly discussed, followed by the YC-15 demonstrator and key technology issues. The rotor design and the CAMRAD II model are covered in some detail. Isolated rotor flutter is discussed, with special attention to the effects of control-system stiffness and model complexity. Whirl mode predictions are included for a variety of flight conditions, based on a reduced-frequency model. The paper concludes with recommendations for improvements to the CAMRAD II model to support further research.

## ATT Concept

The ATT is described in Ref. 1; a brief summary is included here for comparison with the demonstrator. The ATT (Fig. 1) is a large-bodied transport with a partially tilting, forward-swept wing, four large propellers, and minimal tail surfaces. Propellers are used instead of turbofans to keep the wing fully immersed in high-energy flow during takeoff and landing. The propellers are designed with cyclic pitch for control power and blade-load alleviation in non-axial flow (hence it is arguably more accurate to call them "rotors," as will be the case herein).

*Presented at the AHS 4th Decennial Specialist's Conference on Aeromechanics, San Francisco, California, January 21–23, 2004.* 

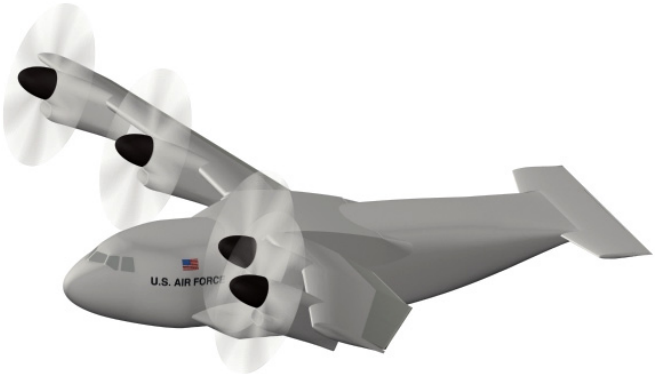

Fig. 1. Full-scale ATT concept.

Table 1 summarizes the ATT characteristics. The SSTOL payload is for a 750-ft takeoff distance; maximum payload requires 1500 ft. The SSTOL payload is an estimated weight of the Army's Future Combat System.

Table 1. ATT Characteristics (full scale)

| | |
|---|---|
| TOGW | 325,000 lb |
| Payload (SSTOL) | 40,000 lb |
| Payload (max) | 80,000 lb |
| Engine (x4) | 11,400 SHP |
| Length | 106 ft |
| Wing Span | 134 ft |
| Prop diameter | 30 ft |
| Ferry range | >5000 nm |
| Max speed | 380 knots |
| Field Length | 750 ft (SLS) |

There are several reasons for the partially tilting wing:

1. Low-speed lift can be achieved with simpler, lighter flaps, partially canceling the weight penalty of the tilt feature.
2. The thrust vector includes a vertical component that directly adds lift.
3. Wing tilt places the thrust line closer to the center of gravity and thereby reduces the pitching moment needed for trim. Because the trim moment is generated by a down force on the tail, any reduction in required moment directly improves takeoff performance.
4. Because the tilted wing is already at a high angle of attack, the fuselage need not be rotated for takeoff. This eliminates the control moment and associated tail download otherwise needed for rotation, again improving takeoff.
5. Ground clearance is increased for the rotor tips and engine intakes.

There are two resultant design characteristics:

1. The wing cannot be structurally integrated with the fuselage, and both structures must support concentrated loads at the hinge and actuator attachments. This increases weight and lowers overall stiffness.
2. To prevent stall, large rotors are needed to provide sufficient flow velocity over the wing and flaps.

These two features—potentially reduced wing stiffness and the large rotors—directly affect whirl-mode stability. This is the motivation for the present research.

## YC-15 SSTOL Demonstrator

The need to rigorously demonstrate performance of the rotor/wing/flap system led to the proposal for a large-scale flight demonstrator (Fig. 2). Table 2 lists key design features. The YC-15 (Fig. 3) was chosen because it is large enough to demonstrate aerodynamics and aeroelastics at nearly full scale (84%), and yet small enough to use existing engines (Rolls-Royce AE 1107C, from the V-22). Also, the YC-15 is capable of demonstrating short-field operations with the Army's Stryker vehicle. The scale of the demonstrator is large enough to represent all critical technology issues for the full-scale ATT.

The YC-15 was originally designed for the Advanced Manned Strategic Transport (AMST) program; its competitor was the YC-14 (Ref. 2). Of the four AMST airframes built, one YC-15 is in better condition than any of the other aircraft, which was a significant factor in its choice for the demonstrator. The YC-15 already has a rear cargo ramp and soft-field landing gear. It also has unusually large tail surfaces, which will increase safety of the demonstration program and allow advanced control features (e.g., cyclic pitch control) to be progressively phased into the test program at a later time.

Significant design features of the YC-15 SSTOL technology demonstrator include:

Partial tilt wing (0-20 deg)
Large props (scaled Hamilton Sundstrand NP2000)
Cross-shafted gearboxes
Fast-moving flaps
Integrated Flight/Prop Controls (IFPC)
Fly-by-wire controls & glass cockpit

Wing tilt is limited to 20 deg to achieve maximum SSTOL performance, which minimizes the weight penalty for tilting the wing and minimizes the low-speed trim requirements. Excessive tilt will stall the wing, even when fully immersed in the rotor flow. The optimum value of wing tilt is reached at a fairly low value of 20 deg. To provide a margin of safety, analyses reported here were conducted for tilt angles up to 30 deg.

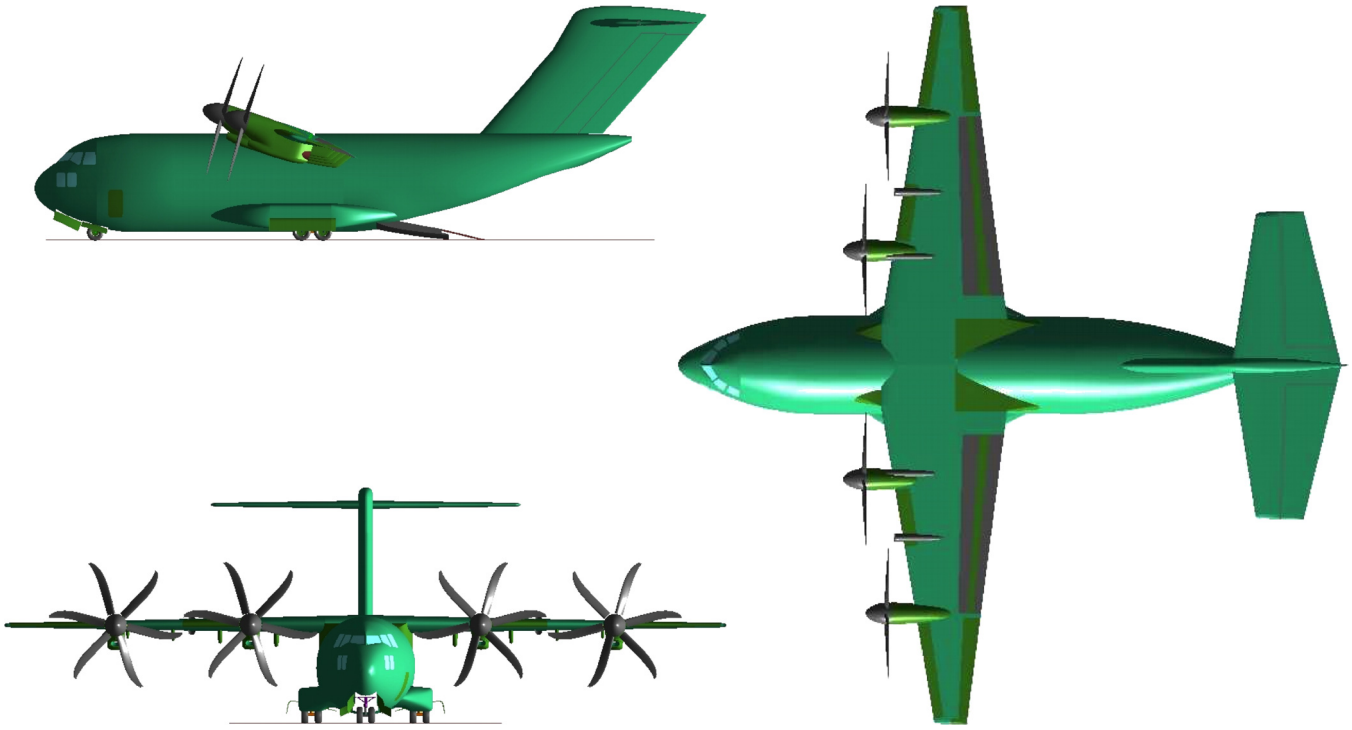

Fig. 2. YC-15 SSTOL technology demonstrator concept.

Table 2. YC-15 SSTOL Design Data

| | |
|---|---|
| TOGW (SSTOL) | 182,000 lb |
| OWE | 124,000 lb |
| Payload (Stryker) | 45,000 lb |
| V-22 Engine (x4) | 6000+ SHP |
| Length | 124 ft |
| Wing Span | 132 ft |
| Wing Tilt | 0-20 deg |
| Prop diameter | 24.5 ft |
| Cruise | .66 M; 30,000 ft |
| Field Length | 750 ft (SLS) |

Fig. 3. YC-15 AMST aircraft.

To limit program cost, not all features proposed for the ATT will be included in the demonstrator. The existing YC-15 landing gear will be used, instead of the more advanced gear proposed for the ATT. Nor will the demonstrator have an advanced cargo-handling system. Some systems will not be installed for initial flight tests, such as cyclic pitch controls. A possible research option for follow-on testing is relaxed stability (simulated small tail), which would be enabled by enhancing the IFPC system to fully exploit the cyclic pitch controls.

### Technology Issues

Several issues require careful analysis and have attracted the attention of NASA because of the potential technology payoffs. These may be summarized under the traditional categories of performance and loads, handling qualities, and aeroelastic stability. Because the last of these directly affects the safety of the airframe structure, and therefore the cost-effectiveness of using the YC-15 SSTOL, it has been given high priority and is accordingly the research focus of this paper.

The YC-15 SSTOL demonstrator must address several critical design issues, including:

Wing tilt (largest airframe to date)
Rotor/wing/flap aerodynamic interaction
Integration of rotor & airframe controls (IFPC system)
Cyclic pitch control

Note that the most conspicuous design feature, the partially tilting wing, is perhaps the least challenging issue. Both variable-sweep and variable-incidence wings have been placed into service in mass-produced military aircraft (e.g., B-1 and F-8), so the technical risk is relatively low. However, a tilting wing must still have adequate stiffness to resist whirl flutter while avoiding excessive weight.

Because it does not hover, the IFPC system should be simpler than that of a VTOL aircraft, such as the V-22, that must transition from wing-borne to thrust-borne controls. Manned simulations of the ATT (Ref. 1) showed that the aircraft can use fixed-wing "stick and throttle" flight controls during SSTOL operation, alleviating the need to transition between flight control modes.

Incorporation of cyclic pitch control to reduce rotor loads and improve control will result in a design unique to both the fixed-wing and tiltrotor experience. This is discussed in more detail in the section entitled Isolated Rotor Flutter.

## Rotor Design Features

Because the rotors proposed for the YC-15 SSTOL have unique design features, they constitute the greatest analytical challenge and are discussed in some detail here. The YC-15 SSTOL rotors have nearly the same diameter as the XV-15's (25 ft), but with over four times the solidity (equal to 0.36 referred to 0.75 $R$). Figure 2 shows a 6-bladed concept, but the most recent concept has 8-bladed rotors. The technology level is the Hamilton Sundstrand NP2000 propeller used on the E2-C (Fig. 4), but with almost double the diameter. The rotors will be modified to have cyclic pitch controls as well as full reversing capability.

Derived from fixed-wing propellers, the demonstrator rotors have no hinges, flexures, or gimbal: in helicopter terms, they are hingeless rotors. Because the blades cannot flap in response to loads, cyclic pitch may be needed to reduce rotor loads. The lack of hinges or gimbal frees enough space for the cyclic-pitch mechanism to be implemented by an internal spider instead of a swashplate, thereby reducing frontal area.

Like all aircraft with tractor rotors, the demonstrator is potentially vulnerable to whirl flutter. Design features expected to affect whirl flutter, compared with existing rotors and propellers, are summarized here:

1. The large total blade area, evident in Fig. 4, combined with high cruise speeds will increase the sensitivity of the rotor to aerodynamic perturbations (the destabilizing forces will be larger).
2. The swept tips should improve the whirl-flutter boundary (Refs. 4 and 5).
3. The rigid hub is beneficial because it eliminates tip-path-plane lag (Ref. 6), but it is potentially detrimental because it strongly couples vertical and lateral nacelle modes via precessional forces (the "whirl" in whirl flutter).
4. The blades' internal construction is different from a tiltrotor. Combined with the unusual (for a tiltrotor) planform, this will lead to different blade modes, hence different modal behavior.
5. The blades are much larger than a conventional propeller. For the same (scaled) stiffness, they will be much heavier, which will again affect the whirl modes.
6. The combination of a rigid hub and cyclic pitch results in blade loads different from either a tiltrotor or conventional propeller, and in potentially different whirl-flutter behavior.
7. Propeller-type pitch bearings are unsuitable for cyclic pitch. Substitution of low-friction bearings (e.g., V-22 elastomeric bearings) will potentially reduce whirl-mode stability.
8. Enclosing the control system inside the shaft and hub will result in different kinematics. Elimination of pitch-flap coupling can be beneficial for stability, compared to a gimballed tiltrotor, but reduction of pitch stiffness (because of shorter pitch horns) can be detrimental.

Fig. 4. Hamilton Sundstrand NP2000 propeller and test stand.

The present paper can only begin to explore the consequences of these design features for aeroelastic stability. Those areas where the YC-15 SSTOL demonstrator differs the most from existing tiltrotors will be emphasized.

One particularly striking example is mentioned here: the current rotor design calls for the blade torsion and flapwise

stiffnesses to vary by some five orders of magnitude from root to tip (Fig. 5). In contrast, the V-22 blade stiffnesses vary by barely two orders of magnitude, at most, and this includes the large variations at the blade fold hinge. The YC-15 SSTOL rotors cannot be expected to exhibit the same aeroelastic behavior as those on any existing rotorcraft.

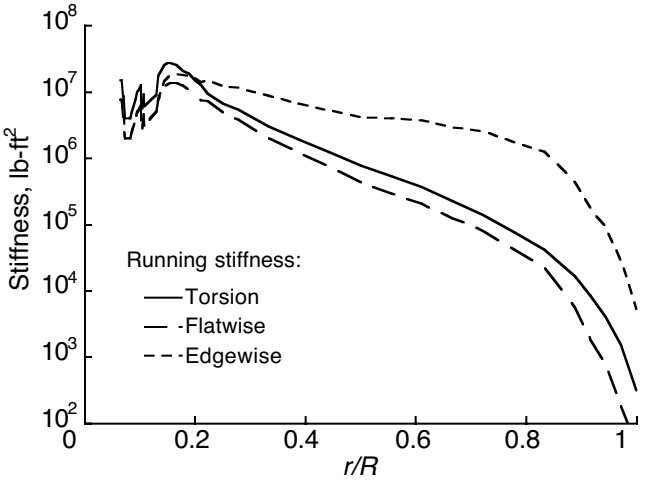


Fig. 5. Scaled NP2000 blade stiffnesses (note semi-log scale).

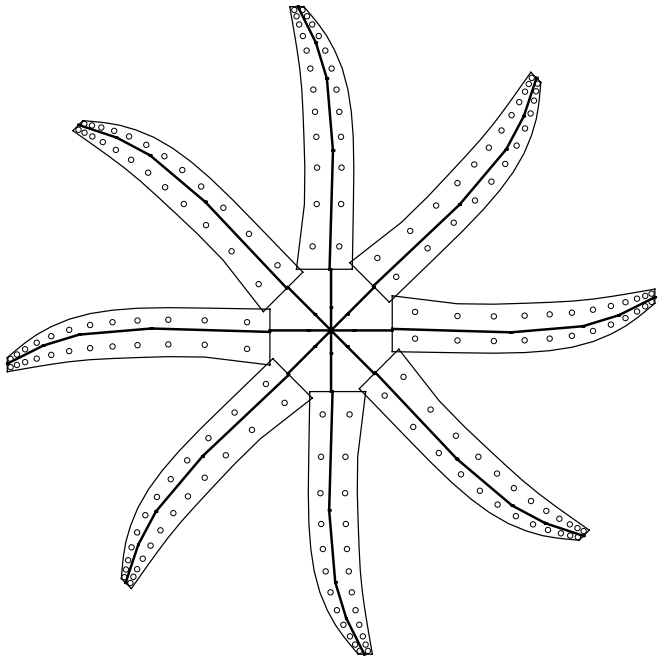

Fig. 6. CAMRAD II model of the ATT demonstrator rotor: solid lines are beam elements, circles are aerodynamic collocation points (compare with Fig. 4).

**CAMRAD II Model**

The YC-15 SSTOL rotor was modeled with CAMRAD II Release 4.2 (Ref. 3). The rotor model is shown in Fig. 6. The model was based on two sources of data: rotor structural and aerodynamic data provided by Hamilton Sundstrand, and airframe data (NASTRAN model) provided by Boeing.

The CAMRAD II structural model included multiple beam elements; details are given below. The aerodynamic model included sweep and unsteady-flow corrections for the aerodynamic panels, plus tip-relief corrections. There were 12 aerodynamic panels with airfoil sections defined at five points; the aerodynamic coefficients varied linearly between the defined points. Each panel had collocation points at 1/4 and 3/4 chord (Fig. 6).

The drive-train model used V-22 engine and gearbox inertias, coupled together with torsionally rigid shafts (hence there were no internal drive-train modes). The gearbox inertias were larger than those expected for the ATT demonstrator, but this was acceptable for the present model.

Because the control-system kinematics have yet to be fully defined, the control-system model was kept as simple as possible. Control stiffness was input as linear torsional stiffness at the blade root, and kept constant for all control settings and for both collective and cyclic modes; the swashplate was not modeled. As discussed below under Isolated Rotor Flutter, this is a potentially serious limitation of the model. The need for careful control-system design is a major motivation for the present research.

To calculate aeroelastic stability, CAMRAD II couples externally generated wing/pylon modes to an internally generated dynamic rotor model. The wing/pylon modes were generated by a NASTRAN semi-span elastic-line model, with boundary conditions adjusted to generate full symmetric and antisymmetric mode shapes. The NASTRAN model was based directly on a YC-15 wing/fuselage model, with C-130 nacelles modified to accept V-22 engines and gearboxes. Zero wing tilt and zero fuel weight were assumed. Hence, there was an implied assumption that the wing tilt mechanism does not substantially affect wing structural dynamics. The NASTRAN model will obviously have to be updated when the design of the wing tilt mechanism is completed.

The analyses assumed zero aerodynamic damping from the wing modes. They also assumed structural damping of 1% critical for all airframe modes. This deliberately underestimated the likely damping of the actual airframe, giving conservative estimates of whirl-flutter boundaries.

A constant-coefficient approximation was used for rotor flutter. This is completely adequate for axisymmetric (axial) flow, and a good approximation for modest amounts of shaft pitch relative to the airflow. Most of the analyses were performed for axisymmetric flow (zero wing tilt). The few nonsymmetric cases are mentioned in context and were limited to 30-deg tilt or less.

For full-airframe whirl-flutter calculations, rotor reactionless modes were not used. They cannot couple with the airframe modes and, therefore, do not affect whirl flutter. For isolated-rotor calculations, rotor reactionless modes were used.

### Trim conditions

For the analyses reported here, the CAMRAD II model was trimmed to either zero power (windmill state) or to thrust to match constant drag area, with the latter referenced to 0.66 M at 30,000 ft. Except where noted, the aircraft was assumed to have zero pitch and yaw angle at the hubs, so that the rotors were in axisymmetric flow. For nonsymmetric trim (tilted wing), the rotor shafts were simply set to a specified pitch angle; the yaw angle was always zero. Airframe aerodynamics were not used for trim. This simple trim model was acceptable for low values of wing tilt and was consistent with the constant-coefficient flutter analysis.

The rotor speed was always 608 rpm, for 780 ft/sec tip speed at a vehicle airspeed of zero knots. Airspeed sweeps were usually terminated at 0.75 M, about 15% above the design cruise speed of 0.66 M. Axisymmetric analyses were performed at both sea level standard (SLS) and 30,000 ft (standard day conditions). Nonsymmetric trim was analyzed at sea level at lower airspeeds, using full power to simulate takeoff and initial climbout.

### Model variations

Two variations of the rotor model were developed: a highly detailed "reference" model and a simplified "research" model. The reference model had six elastic beam elements outboard of the pitch bearing, plus a rigid hub inboard of the bearing. The bearing introduced a localized reduction in bending stiffness, which was modeled as a flap/lag gimbal with very stiff springs. The reference model was as complete a representation of the rotor as possible within CAMRAD II. However, it required excessive CPU time when all four rotors (32 blades total) were analyzed together for stability. This model was used only rarely to generate reference predictions against which to check the research model.

The research model was developed to reduce CPU time. It had four elastic beam elements over the aerodynamic portion of the blade, a rigid hub, and a rigid shank between the pitch bearing and the inboard elastic element. To compensate for the increased shank stiffness, the flap/lag springs were reduced in stiffness. Isolated rotor frequencies were generated for the two models; the results were closely similar for the nine lowest frequencies. The simpler research model was used for all predictions reported herein.

Figure 7 is a fan plot of the frequencies up to the ninth mode, calculated at a collective pitch angle of 40 deg. Of particular interest are the rigid pitch and first elastic torsion modes, at 51 and 122 Hz (for 608 rpm). The intersection of the rigid pitch mode with 5/rev is obviously undesirable; the consequences and cure are discussed below. The intersection of the elastic torsion mode with 12/rev is of less concern because of the much higher frequency.

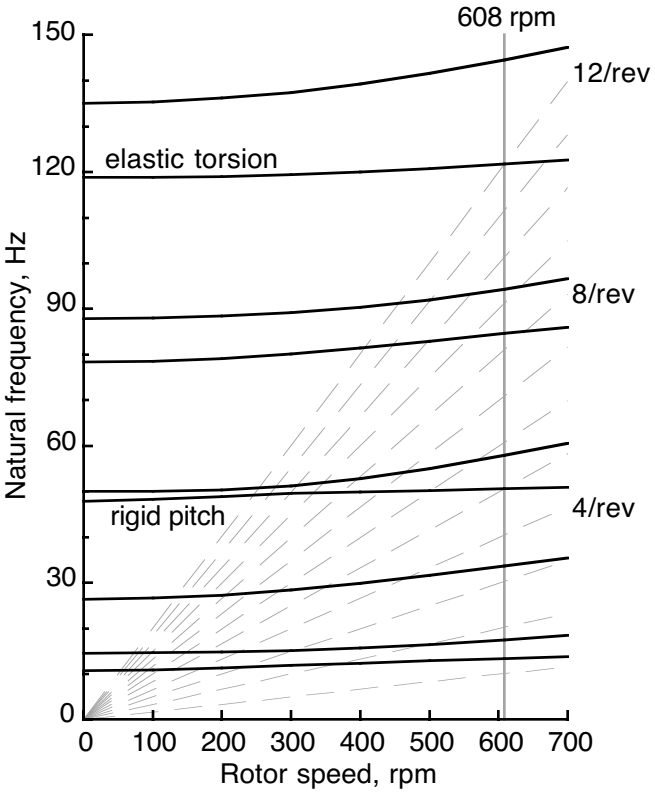


Fig. 7. CAMRAD II predictions of isolated rotor frequencies, at a collective pitch angle of 40 deg (zero bearing friction and damping).

## Isolated Rotor Flutter

### Control-system stiffness

The NP2000 propellers, upon which the ATT demonstrator design is based, rely on high static bearing friction for pitch stiffness. Given that a conventional propeller typically goes through only one full blade-pitch cycle per flight, this is a reasonable design approach. But with cyclic pitch control, each blade will experience several degrees of pitch change each revolution; a high-friction bearing would absorb too much power. Merely scaling up an existing propeller hub and bearing is infeasible. A rotor with cyclic pitch must use low-friction bearings and rely upon the control system to react the pitching moments.

The high-friction bearing has interesting consequences for whirl flutter. As long as there is no significant motion, the effective pitch stiffness is extremely high; in this case, about $10^7$ in-lb/rad. If the blade starts moving in pitch, the stiffness drops to the residual value contributed by the control system,

here about $1.3\times10^6$ in-lb/rad. The bearing friction now contributes damping, not stiffness. Moreover, this is Coulomb damping, not viscous damping, and is inherently nonlinear. If the aerodynamic forces are high enough to force any pitching motion, the amplitude can increase without limit (Ref. 7). Therefore, even high friction damping is no guarantee against flutter.

An exact analysis would require a nonlinear time-series model, whereas CAMRAD II uses a linearized frequency-domain (eigenvalue) analysis for flutter. Because friction damping depends upon both the frequency and amplitude of the motion, it is difficult to linearize with good accuracy within a multi-mode analysis.

For efficiency, the present research took the simple approach of performing frequency-domain analyses of the isolated rotor at two extreme values of stiffness: the nominal maximum value, corresponding to near-zero motion, and the nominal minimum, corresponding to free motion. The second condition assumed zero viscous damping. While neither condition would be met exactly in practice, together they bound the problem. For small motion, friction damping does not change the natural frequency (Ref. 7), so this analytical approach is acceptable. As will be shown, further analyses adjusted the minimum value to avoid flutter.

**Blade flutter predictions**

The resulting flutter predictions for an isolated rotor at zero power are summarized in Fig. 8, which shows the damping of the rigid pitch mode as a function of blade section Mach number at 0.75 $R$. This is the effective Mach number, corrected for local sweep. The forward (axial) airspeed varies from 0.3 to 0.75 M; the upper limit provides a 15% margin over the nominal cruise speed of 0.66 M (maximum speed is 0.7 M, which is 413 knots at 30,000 ft). Only the rigid pitch mode is shown; this is the only unstable mode. The mode is manifest in the fixed system as the fundamental frequency $f$ , $f\pm1$/rev, $f\pm2$/rev and $f\pm3$/rev, for seven modes with similar trends with airspeed. For clarity, only the lowest-frequency mode is plotted.

Note the extreme sensitivity to airspeed, especially from 0.75 to 0.80 M. The airfoil compressibility effects are clearly evident. Figure 8 also shows the damping predictions for the maximum value of pitch stiffness, which assumes that there is no pitch motion. Although extreme stiffness eliminates the low-speed instability, it also eliminates the stabilizing effects of compressibility.

The unstable pitch mode that occurs with minimum pitch stiffness is clearly unacceptable. A simple cure was to assume a slightly higher minimum value; 1.3 times the nominal value proved sufficient to raise the rigid pitch mode above the fourth flap/lag mode (Fig. 7) and eliminate the problem. Stiffening the outer blade also cured the instability, but the required additional stiffness was impracticably large and was not further pursued. At high Mach numbers, compressibility effects dominate the response, which is largely independent of pitch stiffness for free bearing motion.

Because the control system will have to be redesigned in any case to accommodate cyclic pitch, a higher stiffness is a reasonable option. The value chosen here is considerably less than the equivalent V-22 stiffness, so it should be feasible. For all further analyses reported here, the increased minimum stiffness was used.

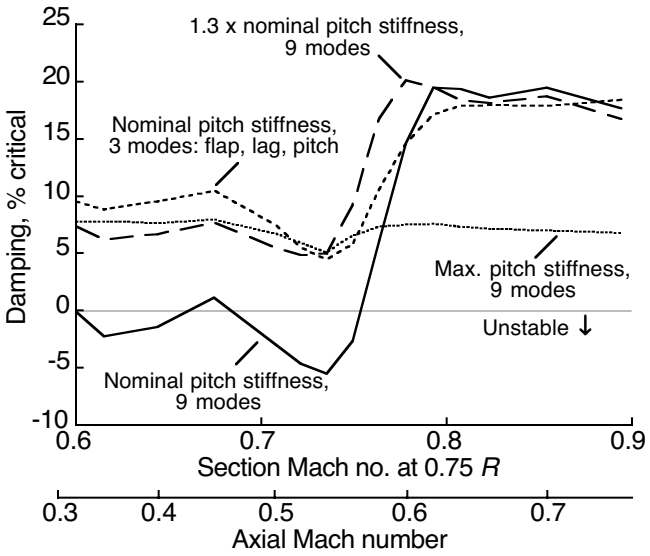


Fig. 8. Damping of isolated rotor blade-pitch mode at zero power, sea level.

A significant finding is that it required blade modes up to the eighth mode (the first elastic torsion mode) to get the correct trends in Fig. 8. The CAMRAD II model added an extra mode, for nine modes total, unless otherwise noted. The "classic" model of first flap, lag and pitch modes was insufficient and did not reveal the instability with nominal pitch stiffness. Progressively adding more modes helped, but it required at least eight modes to get consistent results.

The effects of control-system kinematics were also examined. As previously mentioned, the control system was usually modeled as having a constant torsional stiffness for blade pitch, with no swashplate. To check its adequacy, the constant-stiffness model was replaced by a swashplate model, based on scaled NP2000 pitch-horn kinematics. There were only minor differences in the isolated-rotor frequency or flutter predictions. The constant-stiffness model was used for all further analyses.

As the YC-15 SSTOL design evolves and matures, an expanded version of the swashplate model will eventually be needed for studies of cyclic control. It will then become appropriate to revisit the assumptions of control-system stiffness and bearing damping used in the CAMRAD II model.

### Whirl Mode Predictions

The isolated-rotor model was coupled to an airframe model to generate predictions of aeroelastic instabilities (whirl modes). Symmetric and antisymmetric modes were analyzed separately. The first twelve elastic airframe modes were used for both symmetric and antisymmetric cases, for a total of 24 modes. The rotor model used the pitch stiffness corresponding to free pitch-bearing motion, as adjusted to avoid blade flutter, but assumed no damping from the bearing.

The least stable operating condition for whirl modes is zero power at sea level. With the nominal NASTRAN model, the whirl modes are completely stable at such conditions (Fig. 9). Only the least stable modes with adverse trends are plotted. Only one symmetric wing mode, with in-phase nacelle yaw (the 8th symmetric mode), shows any significant trend towards instability. Two antisymmetric modes have unfavorable trends: fin torsion and wing bending, the latter with out-of-phase nacelle pitch (the 5th and 7th antisymmetric modes, respectively).

Because of the large number of airframe modes, plus the close coupling of nacelle and wing modes, the mode labels in Fig. 9 and the figures below are somewhat arbitrary. Care was taken to track frequencies properly, but no attempt was made to trace all modal contributions to coupled modes as airspeed or other parameters were varied.

Although the nominal model was stable, the compromises in the NASTRAN model (notably, rigid nacelles and no tilt mechanism) motivated investigation of reduced-stiffness models, wherein the frequencies of all airframe modes were reduced by a uniform percentage. Although non-rigorous because the mode shapes and modal masses were not recalculated, this was an efficient method of revealing areas of potential concern.

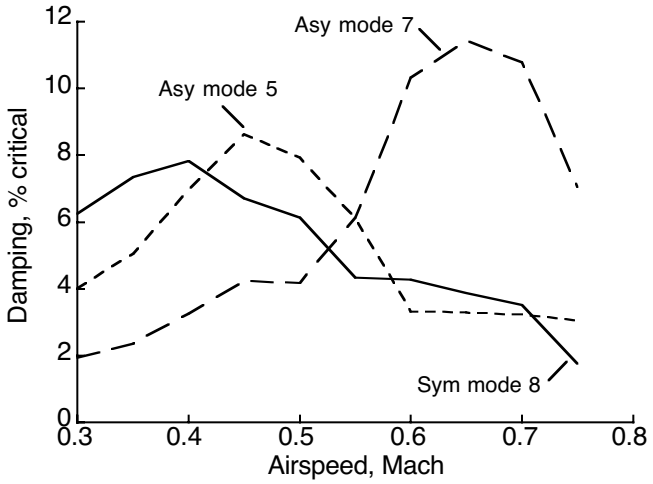


Fig. 9. Damping of the least stable airframe modes for trim to zero power at sea level, nominal NASTRAN frequencies.

With 80% frequencies, the aircraft is barely stable at 0.75 M; with 70% frequencies, it was unstable at 0.75 M. Figures 10 and 11 show the least stable symmetric and antisymmetric modes, respectively, for 70% NASTRAN frequencies. The least stable modes are the same as those with nominal NASTRAN frequencies (Fig. 9). The symmetric nacelle yaw mode (mode 8) is now unstable at very high speeds, as is antisymmetric nacelle pitch (mode 7). A 30% reduction in frequency corresponds to a 50% reduction in stiffness: a very large change, but not out of the question for a design that is a hybrid of components not originally intended for the purpose. This also suggests the potential for weight savings, or at least that provisions for whirl flutter need not add significant weight.

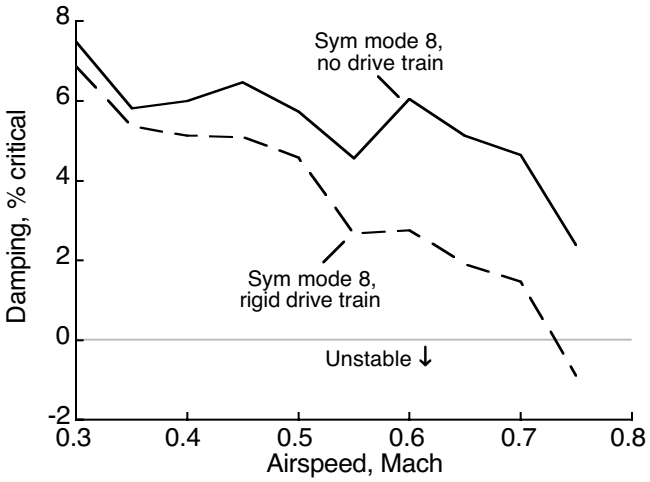


Fig. 10. Damping of the least stable symmetric airframe mode, with and without a drive train, at zero power, sea level, 70% NASTRAN frequencies.

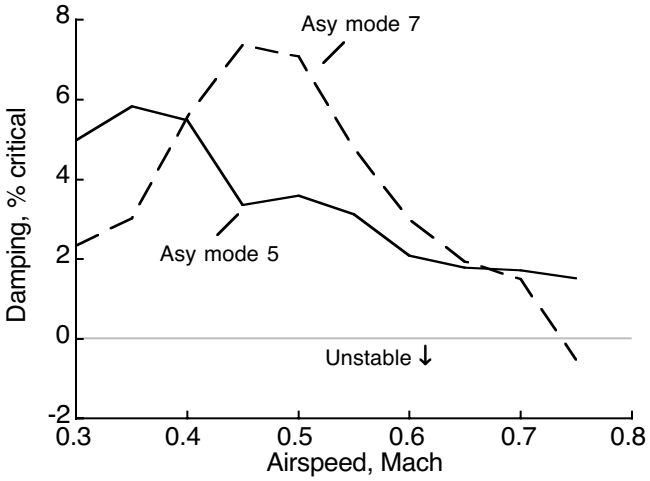


Fig. 11. Damping of the least stable antisymmetric airframe modes, at zero power, sea level, 70% NASTRAN frequencies.

Also shown in Fig. 10 is the effect of the drive train. Ignoring the drive train significantly increased the damping. Because the drive-train model assumed rigid cross-shafts, the antisymmetric modes were unaffected (not shown). The sensitivity to the drive train suggests that the CAMRAD II model should be updated to include details of the cross-shaft and other components as the YC-15 SSTOL design matures.

The next four figures illustrate the effects of altitude and power on whirl flutter, again assuming 70% NASTRAN frequencies to emphasize any flutter sensitivity. Figure 12 shows the modes of Figs. 10 and 11, but for zero power at 30,000 ft (the design cruise altitude). The maximum airspeed analyzed is 0.75 M, where the helical tip Mach number is 1.09 at 30,000 ft; sweep reduces the effective tip section Mach number to 0.89.

For Fig. 13, the aircraft was trimmed to thrust at 30,000 ft altitude; thrust was matched to airframe drag for a constant flat-plate area. Nominal cruise power is reached at 0.66 M. The modes of Figs. 12-13 are now stable, with favorable trends up to 0.7 M or higher; no modes have significant unfavorable trends.

Figure 14 shows damping trends for the aircraft trimmed to thrust at sea level. The vertical and horizontal scales are matched to Figs. 12 and 13, although maximum power is reached at about 0.45 M. The blade pitch mode of the isolated rotor (not shown) becomes unstable at 0.5 M, but is stabilized at higher speeds, consistent with Fig. 8. Because this is an unreachable operating condition, the instability is not limiting.

Figure 15 summarizes the effects of thrust and altitude for the 8th symmetric mode. It is immediately apparent that altitude is stabilizing at the same Mach number. Thrust—or equivalently, power—is stabilizing for high Mach numbers at cruise altitude, and very slightly stabilizing at sea level.

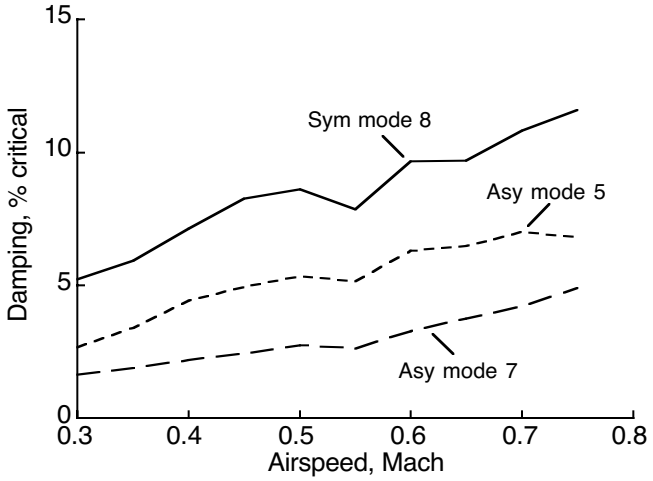


Fig. 12. Damping of the least stable airframe modes for trim to zero power, at 30,000 ft altitude, 70% NASTRAN frequencies.

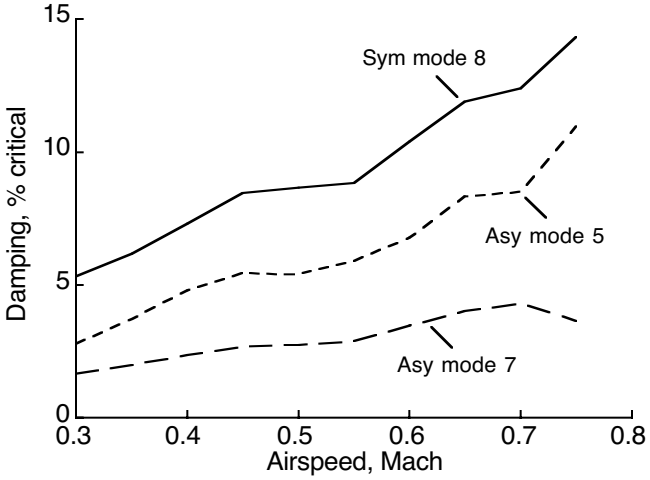


Fig. 13. Damping of the least stable airframe modes for thrust matched to drag, at 30,000 ft altitude, 70% NASTRAN frequencies.

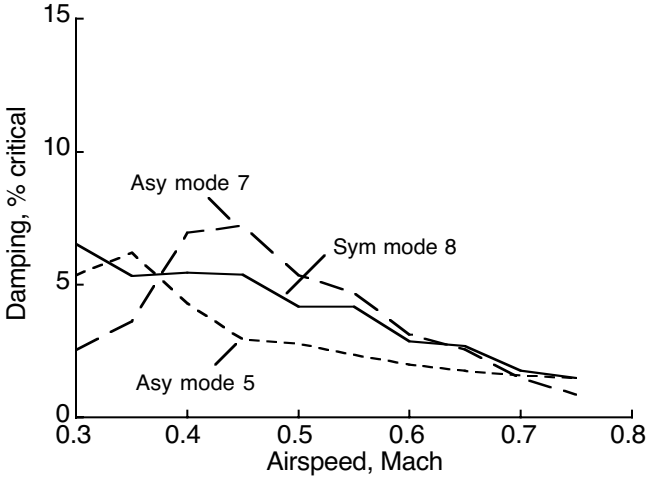


Fig. 14. Damping of the least stable airframe modes for thrust matched to drag, at sea level, 70% NASTRAN frequencies.

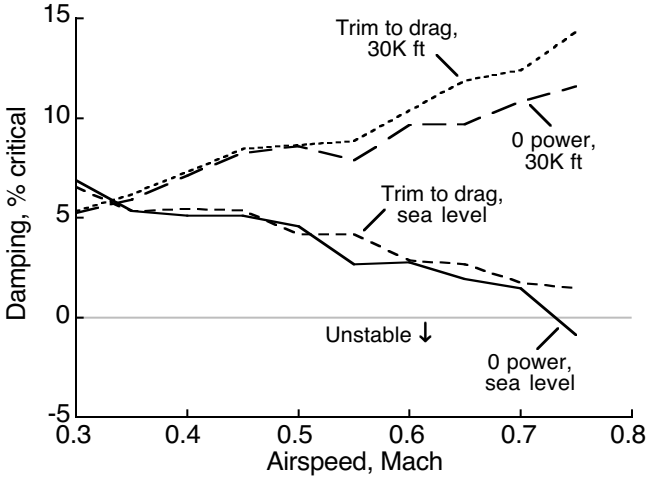


Fig. 15. Effects of thrust and altitude on the 8th symmetric mode, 70% NASTRAN frequencies.

The effects of wing tilt were also examined. Whirl-flutter predictions were performed for wing tilt up to 30 deg. Only the effective rotor pitch was changed; the NASTRAN modes were not recalculated. However, the 70% reduction in NASTRAN frequencies was retained. To simulate takeoff, the aircraft was assumed to be at full power (6000 SHP per rotor) at sea level; maximum airspeed was 0.45 M. Maximum design speed for 20-deg wing tilt is only 0.2 M, so this is a very generous margin. No unstable modes or unfavorable trends were found. Figure 16 shows the trends for the same modes as Figs. 9-15. There is relatively little variation with airspeed, although the airspeeds are lower than in previous figures. The modes shown are not necessarily the least stable, but the less stable modes vary even less with airspeed. The figure illustrates that there are no detrimental effects of wing tilt on whirl-mode stability.

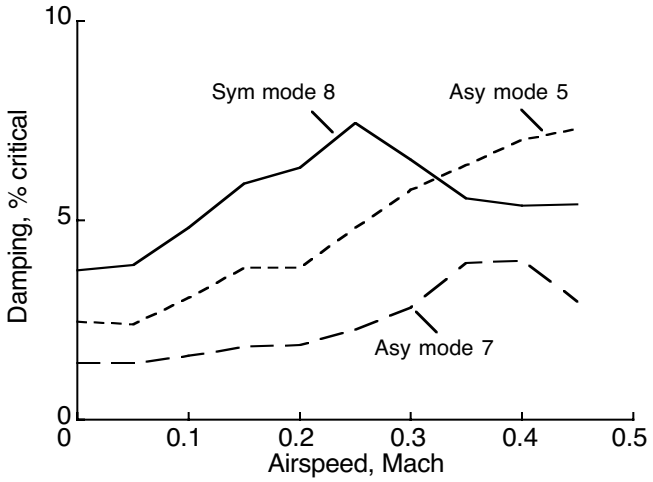


Fig. 16. Damping of the least stable airframe modes at full power, sea level, with 30-deg wing tilt, 70% NASTRAN frequencies.

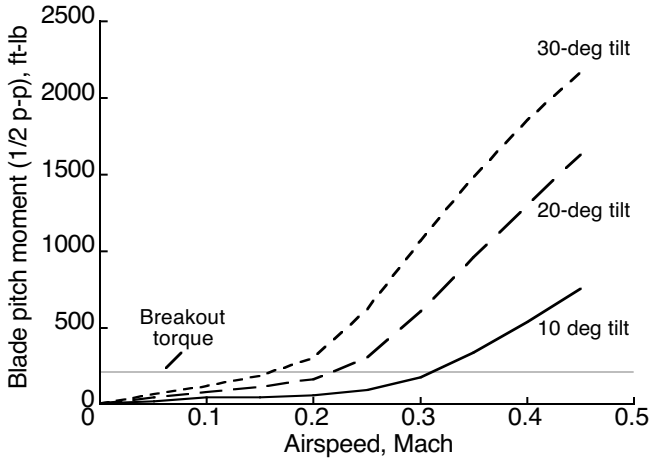


Fig. 17. Blade vibratory pitch moment (1/2 peak-to-peak) at full power, sea level.

The most significant result of tilting the wing was that the half peak-to-peak blade torsion loads could exceed the breakout torque of the blade pitch bearing (Fig. 17), reinforcing the concern that static bearing friction cannot be relied upon to stabilize the blade modes.

## Model Improvements

As the design of the YC-15 SSTOL demonstrator progresses, more detailed data should become available for incorporation into an improved CAMRAD II model. Possible areas of improvement are summarized below.

The airfoil tables were constructed by splicing Hamilton Sundstrand data into XV-15 tables (XV-15 tables were used because the data are in the public domain). The tables could be expanded to provide greater margins for off-design flight conditions, and restructured to eliminate constraints imposed by the XV-15 tables.

The nacelles were modeled in NASTRAN as rigid beams with lumped masses. Flexibly mounted engines and transmissions will obviously affect the modal predictions, as will the inclusion of engine-mount dampers and other design details. The NASTRAN model did not include the wing tilt mechanism. If the load paths near the mechanism remain similar to those of the unmodified YC-15 wing, then the airframe modes will not change significantly, but this has yet to be evaluated. Tilting the wing with respect to the fuselage will change the NASTRAN modes, hence the whirl-flutter predictions, but this applies only to low-speed flight (takeoff and landing) where whirl flutter is not likely to be encountered.

The cyclic control-system design is still at the conceptual design level. The final design is unlikely to have the same kinematics as scaled NP2000 propeller controls. Also, it may be expected that the collective and cyclic control stiffnesses will be different, with consequent effects on whirl flutter. Also, the final pitch-bearing design will affect the total effective control stiffness and damping. All such details should be incorporated into the CAMRAD II model as they become available.

The CAMRAD II model assumed that the rotor blade center of gravity, elastic axis and tension center are all coincident, which will not necessarily be true for the final design. Such details can readily be incorporated into the CAMRAD II model.

## Research Recommendations

With an improved model in hand, per the suggestions above, CAMRAD II analyses should be repeated as necessary to determine the effects of design details on whirl flutter. The effects of blade airfoils, nacelle structure and mass distribution, wing-tilt mechanism, drive-train stiffness and inertia, control-system stiffness and kinematics, and rotor blade structure must all be examined in due course.

Beyond aeroelastic stability, it will be appropriate to calculate blade loads and aerodynamic interference, which imply a wake model. This is a potentially major undertaking because of the complexity of a four-rotor wake model.

## Concluding Remarks

No significant whirl-mode instabilities were discovered during this initial round of analyses. However, the potential for blade flutter exists for the nominal minimum value of blade pitch stiffness, which itself depends upon the assumed pitch-bearing and control-system characteristics. These aspects of the rotor design vary significantly from helicopter and tiltrotor practice, and will have to be examined in more detail as the design of the cyclic controls evolves.

In order to model blade aeroelastic effects, CAMRAD II had to use a far greater number of blade modes than needed for classic tiltrotor analyses. Eight modes were needed to fully capture the trends of blade flutter with Mach number.

There appears to be a generous margin of wing and nacelle stiffnesses: wing/nacelle mode frequencies could be reduced by 30%, equivalent to 50% stiffness reductions, before encountering whirl flutter. Tilting the wing up to 30 deg had no deleterious effects. However, the unusual design of the partial tilt wing, especially at such a large scale, is grounds for caution; further analyses with a more detailed NASTRAN model are certainly warranted.

The YC-15 SSTOL demonstrator should be feasible with existing propeller technology and will open the door to the new vehicle and operational concepts embodied in the ATT.

## Acknowledgements

The authors wish to thank Richard J. Peyran of the U.S. Army for his assistance with the NASTRAN model. David J. Manley of Boeing provided the ATT data and much insight into its design logic. Henry Healy and David Nagle of Hamilton Sundstrand provided the rotor data, and Scott Lile, also of Hamilton Sundstrand, provided the airfoil tables. As always, Wayne Johnson's advice and help with CAMRAD II proved invaluable.

## References

1. Manley, D. J., and von Klein, W., "Design and Development of a Super-Short Takeoff and Landing Transport Aircraft," AIAA-2002-6023, International Powered Lift Conference, Williamsburg, VA, November 5-7, 2002.

2. Norton, B., *STOL Progenitors: The Technology Path to a Large STOL Aircraft and the C-17A*., AIAA, Reston, VA, 2002, pp. 206-207.

3. Johnson, W., "CAMRAD II Comprehensive Analytical Model of Rotorcraft Aerodynamics and Dynamics," Johnson Aeronautics, Palo Alto, California, 2002.

4. Srinivas, V., Chopra, I., and Nixon, M. W., "Aeroelastic Analysis of Advanced Geometry Tiltrotor Aircraft," *Journal of the American Helicopter Society*, Vol. 43, No. 3, July 1998.

5. Acree, C. W. Jr., "Rotor Design Options for Improving V-22 Whirl-Mode Stability," Proceedings 58th Forum of the American Helicopter Society, Montréal, Quebec, Canada, June 11-13, 2002.

6. Hall, W. E., Jr., "Prop-Rotor Stability at High Advance Ratios," *Journal of the American Helicopter Society*, Vol. 11, No. 2, April 1966.

7. Steidel, R. F. Jr., *An Introduction to Mechanical Vibrations*. John Wiley and Sons, New York, NY, 1979, pp. 201-204.; p. 231 ff.